International Journal of Materials Science ISSN 0973-4589 Volume 12, Number 2 (2017)

Spectroscopic investigation (FT-IR, FT-Raman, UV, NMR), Computational analysis (DFT method) and Molecular docking studies on 2-[(acetyloxy) methyl]-4-(2-amino-9h-purin-9-yl)butyl acetate

Fathima Rizwana B.[1], Johanan Christian Prasana[1] and S.Muthu[2*]

[1]Department of Physics, Madras Christian College, Chennai-59, Tamilnadu, India,
[2]Department of Physics, Arignar Anna Govt. Arts College, Cheyyar-604407, Tamilnadu, India.

**E-mail: mutgee@gmail.com*

Abstract

A systematic approach has been adopted for structural analysis of, 2-[(acetyloxy)methyl]-4-(2-amino-9H-purin-9-yl)butyl acetate by FT-IR, FT-Raman, UV and NMR spectroscopic techniques. The optimized molecular geometry, the vibrational assignments, the IR and the Raman scattering activities were calculated by using density functional theory (DFT) B3LYP method with 6-311++G(d,p) basis set. The calculated HOMO and LUMO energies show the charge transfer within the molecule. Stability of the molecule arising from hyperconjugative interactions, charge delocalization have been analyzed using natural bond orbital analysis (NBO). Molecular electrostatic potential (MEP) and Fukui functions calculation were also performed. The thermodynamic properties (heat capacity, entropy, and enthalpy) of the title compound at different temperatures have been calculated. Antiviral activity was examined based on molecular docking analysis and it has been identified that the title compound can act as a good inhibitor against Herpes Simplex Virus.

Key words : DFT, FTIR, NMR, UV-Visible, Docking.

Introduction :

2-[(acetyloxy)methyl]-4-(2-amino-9H-purin-9-yl)butyl acetate is a guanine analogue antiviral drug used for the treatment of various herpesvirus infections, most commonly for chronic delta hepatitis [1] herpes zoster (VZV), herpes simplex virus types 1 (HSV-1) and 2 (HSV-2) [2]. Commonly, 2-[(acetyloxy)methyl]-4-(2-amino-9H-purin-9-yl)butyl acetate is known as Famciclovir (FCV) [3]. It is also indicated for treatment of recurrent episodes of herpes simplex in HIV patients. Famciclovir is the recently licensed oral formulation of the guanosine analogue penciclovir. It is

available in markets under the brand name Famtrex. Famciclovir is absorbed well and converted efficiently to penciclovir, which is a potent inhibitor of viral DNA synthesis. Few spectroscopic studies have been reported on the title compound [4,5].

Structural and bonding features reveal that this FCV molecule has several reactive groups which contribute in both intra and intermolecular hydrogen bonding interactions with biological targets. Literature survey reveals that so far there is no detailed experimental and theoretical study of the title compound. In this present study, we report a detailed spectroscopic investigation of 2-[(acetyloxy)methyl]-4-(2-amino-9H-purin-9-yl)butyl acetate (FCV) using B3LYP/6-311++G(d,p) level of the theory. The FT-IR and FT-Raman spectral analysis of FCV are performed using density functional theory. The redistribution of electron density(ED) in various bonding, antibonding orbitals and E(2) energies are calculated by the natural bond orbital(NBO) investigation. The local reactivity descriptors are obtained with the help of Fukui function calculation. Several properties like molecular geometry, Highest Occupied Molecular Orbital (HOMO) and Lowest Unoccupied Molecular Orbital (LUMO) energies, Nuclear Magnetic Resonance (NMR), UV-Visible, Molecular Electrostatic Potential (MEP) analysis of the FCV gives clear information about charge transfer within the molecule. Antiviral activity was analyzed using molecular docking method.

Experimental details:

The title compound was purchased from sigma Aldrich company with 99% purity, and was used as such without any further purification. The FTIR spectrum of the title compound was recorded in the region 4000-400 cm^{-1} in the evacuation mode using a KBr pellet technique with 1.0 cm^{-1} resolution on a PERKIN ELMER FT-IR spectrophotometer. The FT-Raman spectrum of the title molecule was recorded in the region 4000-100cm^{-1} in a pure mode using Nd:YAG Laser of 100mW with 2cm^{-1} resolution on a BRUCKER RFS 27 at IIT SAIF, Chennai, India. The UV–vis spectrum of the molecule was also recorded by the UV–Visible spectrophotometer in the wavelength region 200–500 nm using DMSO as a solvent. Carbon(^{13}C) NMR and Proton(^{1}H) NMR spectra were recorded on a Bruker AVANCE III 500 MHz (AV 500) multi nuclei solution NMR Spectrometer using DMSO as solvent at 400 MHz at CAS in IIT SAIF, Chennai, India.

Computational method:

Quantum chemical density functional computations were carried out at the Becke3-Lee-Yang-parr (B3LYP)[6] level with 6-311++G(d,p) basis set using Gaussian [7] program package to get a clear knowledge of optimized parameters. The optimized molecular structure is used for the computation of vibrational frequencies, Raman activities and IR intensities with the Gaussian software system molecular visualization program at the same level of theory and basis set. The theoretical vibrational assignments of the title molecule using percentage potential energy distribution (PED)

were done with the VEDA [8] program. Raman scattering activities of the fundamental modes were suitably converted into the relative Raman intensities [9,10]. The electronic properties such as HOMO and LUMO energies were determined. In order to understand the electronic properties, the theoretical UV-Vis spectra have been investigated by TD-DFT method with 6-311++G(d,p) basis set for the gas phase. The ^{1}H and ^{13}C NMR chemical shift were calculated with gauge-including atomic orbital (GIAO) approach [11] by applying B3LYP/6-311++G(d,p) method of the title molecule and compared with the experimental NMR spectra. The NBO analysis and MEP calculations were performed on the title molecule. NBO analysis gives a clear evidence of stabilization originating from hyperconjugation of various intramolecular interactions. The Mulliken population analysis and condensed Fukui functions were reported. Molecular docking (ligandprotein) simulations have been performed by using AutoDock 4.2.6[12] free software package.

Results and discussion:

Molecular geometry:

The bond parameters (bond length and bond angles) of the title molecules are obtained using DFT/B3LYP method with 6-311++G(d,p) basis set and are listed in Table 1. The optimized molecular structure of title compound is shown in Fig. 1. The theoretical calculations were carried out isolated molecule in the gas phase. The homonuclear bonds (C6-C7, C6-C19, C5-C6, C1-C2) have higher bond lengths as 1.541Å, 1.533Å, 1.531Å, 1.513Å respectively and heteronuclear bonds (N18-H36, N18-H37, C5-H27, C10-H34, C23-H42) have less bond lengths as 1.007Å, 1.007Å, 1.094Å, 1.081Å, 1.091Å respectively.

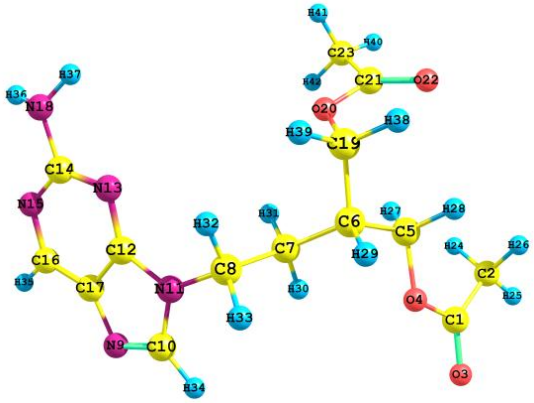

Fig. 1. Optimized geometric structure with atoms numbering of FCV molecule

Table 1. Geometrical parameters optimized in 2-[(acetyloxy)methyl]-4-(2-amino-9H-purin-9-yl)butyl acetate bond length (Å) and bond angle (^{o}) with 6-311++G(d,P) basis set.

Bond Length(Å)	B3LYP/6-311++G(d,p)	Bond Angle(°)	B3LYP/6-311++G(d,p)
C1-C2	1.513	C2-C1-O3	123.9
C1-O3	1.201	C2-C1-O4	117.8
C1-O4	1.364	C1-C2-H24	111
C2-H24	1.093	C1-C2-H25	108.2
C2-H25	1.087	C1-C2-H26	111.5
C2-H26	1.093	O3-C1-O4	118.3
O4-C5	1.44	C1-O4-C5	122.1
C5-C6	1.531	H24-C2-H25	109.2
C5-H27	1.094	H24-C2-H26	107.4
C5-H28	1.092	H25-C2-H26	109.5
C6-C7	1.541	O4-C5-C6	106.7
C6-C19	1.533	O4-H5-C27	110
C6-H29	1.099	O4-C5-H28	110.3
C7-C8	1.534	C6-C5-C27	111
C7-H30	1.092	C6-C5-H28	110.3
C7-H31	1.094	C5-C6-C7	111.7
C8-N11	1.459	C5-C6-C19	111.4
C8-H32	1.091	C5-C6-H29	105.9
C8-H33	1.094	H27-C5-H28	108.5
N9-C10	1.304	C7-C6-C19	113.2
N9-C17	1.387	C7-C6-H29	108.8
C10-N11	1.39	C6-C7-C8	112.9
C10-H34	1.081	C6-C7-H30	108.8
N11-C12	1.374	C6-C7-H31	109.7
C12-N13	1.327	C19-C6-H29	105.4
C12-C17	1.409	C6-C19-O20	112.5
N13-C14	1.344	C6-C19-H38	111
C14-N15	1.354	C6-C19-H39	110.5

Vibrational Assignments:

The maximum number of potentially active observable fundamentals of the non-linear molecule, which contains N atoms, is equal to (3N-6) apart from three translational

and three rotational degrees of freedom [13,14]. The title molecule consists of 42 atoms, which has 120 normal modes of vibration. The comparative theoretical and experimental FT-IR and FT-Raman spectra are shown in Figs. 2 and 3. The spectral assignments of selective modes with PED contributions are tabulated in Table 2.

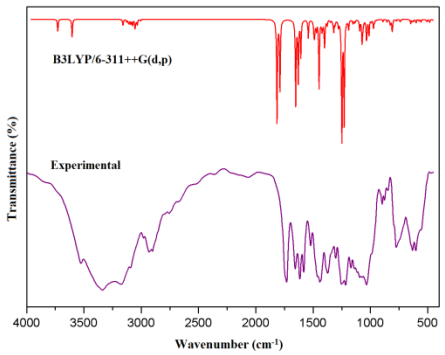

Fig. 2. Compared FT- IR spectra of FCV

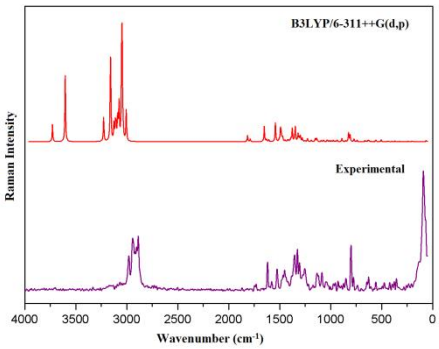

Fig.3. Compared FT-Raman spectra of FCV

C-H vibrations:

Aromatic compounds commonly exhibit multiple weak bands in the region of 3100–3000 cm^{-1} due to the aromatic C-H stretching vibrations. They are not appreciably affected by the nature of the substituent [15-18]. The calculated C-H stretching vibrational modes of the FCV molecule were obtained at 3120 and 3056 cm^{-1}. The observed peaks at 3132, 3066 cm^{-1} in FT-Raman spectrum and 3174, 3093 cm^{-1} in FT-IR spectrum were assigned to the C-H stretching vibrations of the molecule. The bands due to the C-H bending vibrations are observed in the region of 1000–1300 cm^{-1} [19,20]. The calculated C-H bending vibrations coupled with other vibrational modes were obtained at 1440 and 1303 cm^{-1}. Correspondingly, the peaks were observed at 1452, 1307 cm^{-1} in FT-Raman and at 1440, 1303 cm^{-1} in FT-IR spectrum.

C-N vibrations:

The C-N stretching usually lies in the region of 1400–1200 cm^{-1} [21]. In the present work, the calculated C-N stretching vibrational modes coupled with certain other vibrations were obtained at 1597, 1575, 1554, 1332, 1311, 1251 and 1095 cm^{-1}. The corresponding modes were observed at 1620, 1579, 1526, 1327, 1307, 1255, 1087 cm^{-1} in FT-Raman spectrum and 1615, 1582, 1521, 1251, 1073 cm^{-1} in FT-IR spectrum. The C-N bending vibrational mode was observed at 488 cm^{-1} theoretically. The corresponding vibrational mode is observed at 475 cm^{-1} in FT-Raman spectrum and 473 cm^{-1} in FT-IR spectrum.

Table 2. Observed and calculated vibrational frequency of the title compound at B3LYP method with 6-311++G(d,P) basis set.

Modes no.	Experimental (cm^{-1})		Calculated Frequencies (cm^{-1})	IR intensity		Raman intensity		Vibrational assignment PED(100%)
	FT-Raman	FT-IR	Scaled	rel	abs	rel	abs	
1	3601	3525	3605	48	10	52	26	STRE NH(100)
3	3132	3174	3120	0	0	73	36	STRE CH(99)
4	3066	3093	3056	15	3	162	80	STRE CH(94)
12	2980	2979	2985	3	1	52	25	STRE CH(94)
14	2942		2953	35	8	13	6	STRE CH(92)
17		2931	2943	4	1	147	72	STRE CH(93)
18	2904		2934	22	5	11	5	STRE CH(92)
19	2888	2901	2906	6	1	94	46	STRE CH(96)
20	1871	2071	1756	410	90	19	9	STRE OC(88)
21	1731	1731	1730	280	61	8	4	STRE OC(86)
22	1620	1615	1597	339	74	47	23	STRE NC(38) BEND NCC(12)
23	1579	1582	1576	244	53	7	3	STRE NC(18) BEND HNH(63)
24	1526	1521	1554	146	32	6	3	STRE NC(25) BEND CNC(17)
27	1452		1452	5	1	1	1	BEND HCH(80)
30		1440	1440	14	3	6	3	BEND HCH(73) TORS HCCO(19)
37		1372	1374	38	8	5	2	BEND HCN(19) TORS HCNC(11)
39	1355		1356	32	7	2	1	STRE NC(32)
43	1327		1332	21	5	40	20	STRE NC(12) BEND HCN(17) TORS HCNC(21)
45	1307	1303	1303	8	2	45	22	BEND HCC(36)
49	1255	1251	1255	2	0	17	9	BEND HCN(26) BEND HCC(11)
51		1216	1213	56	12	2	1	STRE OC(36) BEND OCC(10)
54	1174	1170	1186	24	5	6	3	STRE NC(22) BEND HCN(44)
55	1135	1139	1151	36	8	5	2	TORS HCCN(14)
56		1114	1114	15	3	9	5	
57	1087	1093	1101	10	2	9	4	STRE CC(12) BEND HCO(11) TORS

								HCOC(14)
58		1073	1095	6	1	3	2	BEND CNC(11) BEND HNC(11)
59	1045		1057	41	9	4	2	STRE NC(11) STRE OC(11) BEND HNC(24)
61		1033	1034	22	5	4	2	STRE OC(12) BEND HNC(15) BEND NCN(10)
63	1004		1023	7	1	0	0	BEND HCH(21) TORS HCCO(50) OUT OCO(29)
67	956		960	8	2	3	2	STRE CC(22) STRE OC(11)
71	875	897	904	2	0	5	2	STRE CC(27) TORS HCOC(23)
72	851	847	861	9	2	9	5	STRE CC(21)
74	801		826	6	1	1	1	TORS HCNC(80)
77	777		784	33	7	19	9	STRE NC(25) BEND NCN(11)
78		774	781	20	4	1	1	TORS CNC(29) TORS NCN(18) OUT NNN(17) OUT NNC(21)
79	738		747	6	1	8	4	BEND HCC(16) TORS HCCN(14) TORS HCNC(14)
81	646		709	2	0	0	0	TORS CNC(32) OUT NNN(42) OUT NNC(11)
82	629	632	643	1	0	3	1	BEND CCO(10) BEND OCC(16) OUT CCC(11)
85		602	605	8	2	4	2	BEND CNC(14) BEND NCN(14)
87	558	556	557	6	1	1	0	TORS HCCO(30) OUT OCO(56)
91	475	473	488	9	2	5	3	BEND NCC(19) BEND NCN(12)
98	356		358	217	47	2	1	BEND NCN(47) BEND CNC(10)
100	283		314	16	4	1	0	BEND COC(13) BEND CCO(12) TORS CNC(19)
102	236		247	1	0	1	0	BEND COC(12) BEND CCC(15) TORS CNC(11)
104	209		198	1	0	1	0	BEND CNC(31)
111	92		97	3	1	0	0	TORS HCCO(10) TORS CCO(47)

C-O vibration:

The carbonyl (C=O) stretching vibrations are the most characteristic vibrations of the IR and Raman spectra, which occur in the region of 1725±65 cm^{-1}. The calculated C=O stretching vibration of the molecule was obtained at 1752, 1730 cm^{-1} and was observed at 1871,1731 cm^{-1} and 2071,1731 cm^{-1} in FT-Raman and FT-IR spectrum respectively. The calculated C=O bending vibrational modes coupled with other vibrations were identified at 643,557 cm^{-1} [22,23]. Correspondingly, the peaks were observed at 629, 558 cm^{-1} and 632, 556 cm^{-1} in FT-Raman and FT-IR spectrum respectively.

C-C vibration:

The C-C stretching vibrations of the title molecule was observed at 1101, 904, 861 cm^{-1} theoretically [24,25]. Correspondingly the peaks were identified at 1087, 875, 851 cm^{-1} in FT-Raman and at 1093, 897, 847 cm^{-1} in FT-IR spectrum. The C-C bending vibrational mode was obtained at 643 cm^{-1} and was observed at 629 cm^{-1} and 632 cm^{-1} in FT-Raman and FT-IR spectrum respectively.

N-H vibration:

In this title molecule, the N-H stretching vibrational mode is calculated at 3605 cm^{-1} and are observed at 3601 cm^{-1} and 3525 cm^{-1} in FT-Raman and FT-IR spectrum respectively. Normally, the NH in plane bending vibrational modes are coupled with the ring stretching and C–NH stretching vibrations and usually occur in the wavenumber region 1650–1500 cm^{-1} [26,27]. In the title molecule, the calculated N-H bending vibrational modes coupled with certain other vibrational modes were predicted at 1576, 1255 cm^{-1}. The corresponding vibrational modes were observed at 1579, 1255 cm^{-1}in FT-Raman spectrum and at 1582, 1251 cm^{-1}in the FT-IR spectrum.

NBO Analysis:

NBO (Natural Bond Orbital) investigation provides an efficient technique to study intra and inter molecular bonding and interaction among bonds, and also provides a convenient basis for investigation charge transfer or conjugative interactions in molecular system [28]. Another useful aspect of NBO method is that it gives information about interactions in both filled and virtual orbital spaces that could improve the investigation of intra and intermolecular interactions. The second order Fock matrix was carried out to evaluate the donor acceptor interactions in the NBO analysis [29]. NBO studies provide the most precise possible ‘natural Lewis structure’ picture of φ because all orbital details are mathematically chosen to include the highest possible percentage of the electron density.

Table 3. Second order perturbation theory analysis of Fock matrix in NBO basis for the title compound.

Donor(i)	Type	ED/e	Acceptor(i)	type	ED/e	[a]E(2)	[b]E(j)-E(i)	[c]F(I,j)
C5-H27	σ	1.89167	C2-H25	σ*	0.00711	0.73	0.9	0.023
			C21-O22	π*	0.32542	21.7	0.45	0.094
N9-C10	π	1.83788	C12-C17	π*	0.47022	20.75	0.25	0.07
N11-C12	σ	1.98352	C8-N11	σ*	0.02961	0.64	1.08	0.024
			N9-C10	σ*	0.01793	0.62	0.92	0.021
			C10-N11	σ*	0.02114	0.59	1.08	0.023
			C10-H34	σ*	0.00523	1.63	1.16	0.039
			C12-N13	σ*	0.01925	0.72	1.25	0.027
			C12-C17	σ*	0.03595	0.59	1.29	0.025
			N13-C14	σ*	0.03736	1.58	1.25	0.04
			C16-C17	σ*	0.03013	1.86	1.29	0.044
C12-C17	π	1.56488	N9-C10	π*	0.43245	20.78	0.17	0.054
			N13-C14	π*	0.33686	13.9	0.24	0.053
			N15-C16	π*	0.27976	24.6	0.26	0.074
N13-C14	π	1.79662	C12-N13	σ*	0.01925	0.63	0.8	0.021
			C12-C17	π*	0.47022	21.87	0.32	0.08
N15-C16	π	1.80195	C12-C17	π*	0.47022	10.17	0.31	0.054
			N13-C14	π*	0.33686	17.73	0.29	0.066
C21-O22	π	1.9346	O4-C5	σ*	0.11011	10.2	0.81	0.082
			C5-H27	σ*	0.05791	6.62	0.83	0.066
O3	LP(2)	1.8574	C1-C2	σ*	0.06934	18.54	0.64	0.099
			C1-O4	σ*	0.09552	30.66	0.66	0.128
O4	LP(2)	1.86299	C1-O3	π*	0.15141	16.44	0.43	0.075
N11	LP(1)	1.55007	C12-C17	π*	0.47022	29.63	0.28	0.082
			N9-C10	π*	0.43245	47.68	0.18	0.084
N13	LP(1)	1.88704	C14-N15	σ*	0.06478	13.63	0.66	0.086
N18	LP(1)	1.87887	N13-C14	σ*	0.03736	6.68	0.72	0.063
			N13-C14	π*	0.33686	11.01	0.22	0.047
O20	LP(2)	1.77422	C21-O22	π*	0.32542	51.21	0.31	0.115
O22	LP(2)	1.81896	O4-C5	σ*	0.11011	17.51	0.71	0.101
			O20-C21	σ*	0.08159	19.11	0.73	0.108
			C21-C23	σ*	0.04391	16.24	0.74	0.101

[a]$E^{(2)}$ means energy of hyper conjugative interaction (stabilization energy)
[b]Energy difference between donor and acceptor i and j NBO orbitals.
[c]F(i,j) is the Fock matrix element between i and j NBO orbitals

For each donor NBO (i) and acceptor (j), the stabilization energy E(2) associated with I, j delocalization can be estimated as,

$$E_2 = \Delta E_{ij} = q_i \frac{F(i,j)^2}{(E_i - E_j)}$$

where q_i is the donor orbital occupancy, E_i and E_j are diagonal elements and F(i,j) is the off diagonal NBO Fock matrix elements.

The larger the E(2) value, the intensive is the interaction between electron donors and electron acceptors [30]. The strong intramolecular hyper conjugative interaction of the σ and π electrons of C-C to the anti C-C bond of the ring leads to stabilization of some part of the ring as evident from Table S3. In the FCV molecule, the interactons between the lone pair LP(2) of O20 with π^*(C21-O22) have the highest E(2) value around 51.21 kJ/mol. The other significant interactions giving stronger stabilization energy value of 47.68kcal/mol to the structure are the interactions between anti bonding of (N9-C10) between the lone pair LP(1) of N11 . The intermolecular hyper conjugative interaction of π (N13-C14) and π * (C12-C17) leading to strong stabilization of 21.87kcal/mol. The strong intramolecular hyperconjugative interaction of σ(N11-C12) distributes to σ^*(C8-N11, N9-C10, C10-N11, C10-H34, C12-N13, C12-C17, N13-N14 and C16-C17) of the ring are shown in the Table 3. On the other hand, side the π(C12-C17) in the ring conjugate to the antibonding orbital of π^*(N9-C10, N13-C14 and N15-C14) which leads to strong delocalization of 20.78, 13.9 and 24.6 kJ/mol respectively.

Fukui functions:

The Fukui function (FF) is one of the extensively used local density functional descriptors to describe chemical reactivity and selectivity. The Fukui function is a local reactivity descriptor that indicates the preferred regions where a chemical species will change its density when the number of electrons is modified. Therefore, it indicates the propensity of the electron density to deform at a given position upon accepting or donating electrons [31-33]. In addition, it is possible to define the corresponding condensed or atomic Fukui functions on the r^{th} atom site for an electrophilic $f^-(r)$, nucleophilic $f^+(r)$ or free radical attack $f^o(r)$, respectively, on the reference molecule as:

$$f^+(r) = q_r(N+1)-q_r(N)$$

$$f^-(r) = q_r(N)-q_r(N-1)$$

$$f^o(r) = [q_r(N+1)-q_r(N-1)]/2$$

In these equations, q_r is the atomic charge (evaluated from Mülliken population analysis, electrostatic derived charge, etc.) at the r^{th} atomic site in the neutral (N), anionic (N+1) or cationic (N–1) chemical species [34]. It contains almost all information about hitherto known different global and local reactivity and selectivity descriptors, in addition to the information regarding electrophilic/nucleophilic power of a given atomic site in a molecule. Dual descriptor (Δf (r)) [35], which is defined as

the difference between the nucleophilic and electrophilic Fukui function and is given by:

$$\Delta f(r)= f^{+}(r) - f^{-}(r)$$

Table 4.Condensed fukui function f_r and new descriptor $(sf)_r$ for the title compound

Atoms	f_r^+	f_r^-	f_r^0	**Δf**	$s_r^- f_r^-$	$s_r^+ f_r^+$	$s_r^0 f_r^0$
C1	0.014951	0.005211	0.010081	0.00974	0.001085	0.003114	0.0021
C2	-0.032285	-0.049904	-0.0410945	0.017619	-0.0104	-0.00672	-0.00856
O3	0.045543	0.029516	0.0375295	0.016027	0.006148	0.009487	0.007817
O4	0.034177	-0.01324	0.0104685	0.047417	-0.00276	0.007119	0.002181
C5	-0.020747	0.012627	-0.00406	-0.033374	0.00263	-0.00432	-0.00085
C6	0.046467	0.009728	0.0280975	0.036739	0.002026	0.009679	0.005853
C7	-0.061683	-0.162492	-0.1120875	0.100809	-0.03385	-0.01285	-0.02335
C8	0.058963	0.061013	0.059988	-0.00205	0.012709	0.012282	0.012496
N9	0.103082	0.085479	0.0942805	0.017603	0.017805	0.021472	0.019639
C10	0.057754	0.103691	0.0807225	-0.045937	0.021599	0.01203	0.016814
N11	-0.002127	-0.035286	-0.0187065	0.033159	-0.00735	-0.00044	-0.0039
C12	0.006844	-0.002455	0.0021945	0.009299	-0.00051	0.001426	0.000457
N13	0.047	0.056169	0.0515845	-0.009169	0.0117	0.00979	0.010745
C14	0.001061	0.010637	0.005849	-0.009576	0.002216	0.000221	0.001218
N15	0.056978	0.06575	0.061364	-0.008772	0.013696	0.011869	0.012782
C16	0.051488	0.112002	0.081745	-0.060514	0.02333	0.010725	0.017027
C17	-0.040673	-0.05804	-0.0493565	0.017367	-0.01209	-0.00847	-0.01028
N18	0.063981	0.020373	0.042177	0.043608	0.004244	0.013327	0.008785
C19	-0.045174	-0.06215	-0.053662	0.016976	-0.01295	-0.00941	-0.01118
O20	0.041359	0.014894	0.0281265	0.026465	0.003102	0.008615	0.005859
C21	-0.004308	0.070435	0.0330635	-0.074743	0.014672	-0.0009	0.006887
O22	0.000416	0.001587	0.0010015	-0.001171	0.000331	8.67E-05	0.000209
C23	0.030536	-0.003829	0.0133535	0.034365	-0.0008	0.006361	0.002782

The dual descriptors $\Delta f(r)$ provide a clear difference between the nucleophilic and electrophilic attack at a particular site with their sign. If $\Delta f(r) > 0$, the site is favored for a nucleophilic attack, whereas, if $\Delta f(r) < 0$, the site may be favored for an electrophilic attack. Fukui functions and local softness for all the atomic sites in the title compound have been listed in Table 4. According to the dual descriptor conditions, the nucleophilic sites for the title compound are C1, C2, O3, O4, C6, C7, N9, N11, C12, C17, N18, C19, O20 and C23. Similarly, the electrophilic attack sites are C5, C8, C10, N13, C14, N15, C16, O21 and O22. The results show that the FCV compound has more biological activity.

Molecular electrostatic potential

MEP is related to the electronic density and is a very useful descriptor in determining sites for electrophilic and nucleophilic reactions as well as hydrogen bonding interactions [36,37]. Molecular electrostatic potential mapping is very useful in the investigation of the molecular structure with its physiochemical property relationships [38,39].

MEPs map of the FCV generated at the optimized geometry of the title molecule using Argus lab program is shown in Fig. 4. The various values of the electrostatic potential are represented by various colors; red represented the regions of the most negative electrostatic potential, white represents the regions of the most positive electrostatic potential. It can be seen that the negative regions are mainly over the oxygen and nitrogen atoms. Negative and positive regions of electrostatic potential are associated with electrophilic and nucleophilic reactivity. The negative molecular electrostatic potential resembles to an attraction of the proton by the evaluate electron density in the molecule, the positive electrostatic potential corresponds to the repulsion of the protons by the atomic nuclei. According to these calculated results, the MEP map illustrates that the negative potential sites are on oxygen and nitrogen atoms and the positive potential sites are around the hydrogen atoms. These active sites found to be clear evidence of biological activity in the title compound.

Frontier Molecular Orbitals

The highest occupied molecular orbital (HOMO) and lowest unoccupied molecular orbital (LUMO) are used to determine the molecular interactions with other species. The energy difference between HOMO and LUMO, called as band gap energy, plays an important role in determining the chemical stability and reactivity of the molecule [40]. The HOMO and LUMO values are related to the Ionization potential and Electron affinity of the molecule. Table 5 shows the values of global molecular reactivity descriptors such as ionization potential (IP), electron affinity (EA), electronegativity (χ), hardness (η), softness (S), chemical potential (μ) and electrophilicity index (ω) predicted for the title molecule. The simulated FMOs are shown in Fig. 5,which indicate the presence of intramolecular charge transfer (ICT) within the molecule. The band gap energy value of the title molecule was calculated as 4.8 eV, which confirms that the molecule has stable structure and the band gap energy value was comparable to the band gap energy value of the bioactive molecules [41].

By using HOMO and LUMO energy values for a molecule, electronegativity and chemical hardness, chemical potential, chemical softness and electrophilicity index can be calculated. The Ionization Potential value indicates that the energy value of 6.12 eV is required to remove an electron from the HOMO. The lower value of Electron Affinity (1.32 eV) indicates that the title compound readily accepts electrons to form bonds; this indicates the higher molecular reactivity with nucleophilies. The higher hardness and lower softness values confirm the higher molecular hardness

associated with the molecule. The lower chemical potential and higher electrophilicity index values identified are comparable with that of the bioactive molecules [42].

Table 5. Calculated energy values of FCV

Basis set	**B3lyp/6-311++G(d,p)**
E_{HOMO}(ev)	-6.1199
E_{LUMO}(eV)	-1.3195
Ionization potential	6.1199
Electron affinity	1.3195
Energy gap	4.8004
Electronegativity	3.7197
Chemical potential	-3.7197
Chemical hardness	2.4002
Chemical softness	0.2083
Electrophilicity index	2.8821

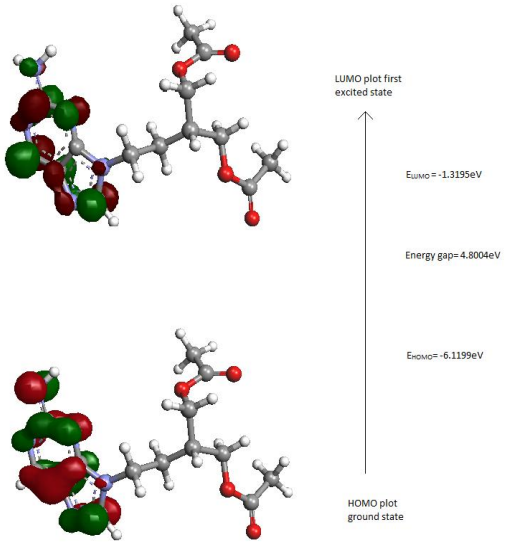

Fig. 5. Frontier molecular orbital for FCV

UV-VIS spectral analysis

The experimental UV-Visible spectrum of FCV molecule is shown in Fig. 6. The theoretical excitation energies, absorption wavelength and oscillator strength were calculated by TD-DFT method with 6-311++G(d,p) basis set. All the calculations were performed assuming the title compound was in liquid phase with DMSO as solvent. The experimental and calculated results of UV-Visible spectral data were listed in Table 6. Experimentally measured λ_{max} values 337, 332, 278 nm showed a good agreement with the theoretical wavelengths 349, 347, 302 nm. The UV-Visible spectral analysis indicates that the electron absorption corresponds to the transition from the ground sate to the first excited state [43,44]. It is mainly described by an electron excitation from highest occupied molecular orbital (HOMO) to the lowest occupied molecular orbital (LUMO). The band gap energy was calculated using the formula $E = hc/\lambda$, here 'h' and 'c' are constants; λ is the cut-off wavelength. Energy gap of title molecule is calculated experimentally by UV-Visible spectrum is 4.4716 eV, Energy gap is calculated theoretically by TD-DFT method is 4.12 eV and from HOMO-LUMO diagram is 4.8 eV.

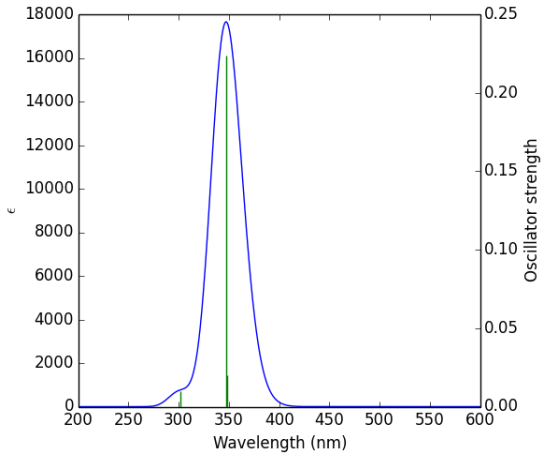

Fig. 6. Theoretical UV–Vis spectra of FCV

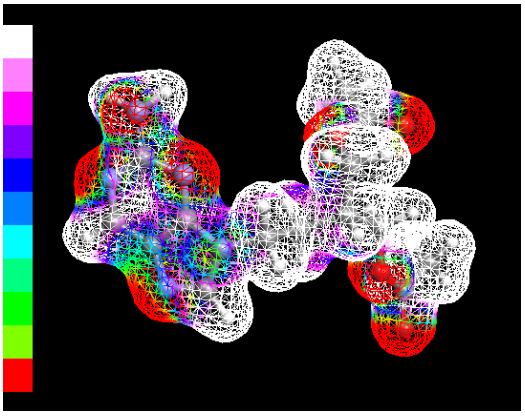

Fig. 4. Molecular electrostatic potential map of FCV

Table 6. UV-vis band gap energy E (eV) and oscillator strength (f) for the title compound

Experimental		Theoretical				Assignments
λ_{max} (nm)	Band gap (eV)	λ_{max} (nm)	Band gap (eV)	Energy (cm^{-1})	f	
337	3.6888	348.28	3.5693	28712	0.0202	H-1->LUMO (21%), HOMO->L+2 (61%)
332	3.7443	347.11	3.5813	28809	0.2235	H-1->LUMO (74%), HOMO->L+2 (17%)
278	4.4716	301.73	4.12	33142	0.0099	H-4->LUMO (13%), H-2->LUMO (45%), H-1->L+1 (22%)

NMR spectral analysis

The experimental and theoretical chemical shift values for carbon (^{13}C) and proton (^{1}H) NMR of the title compound are given in Table 7. The experimental ^{13}C and ^{1}H NMR spectra were recorded in a liquid phase using DMSO-d6 as the solvent and are shown in Figs. 7 and 8. The isotropic chemical shifts are frequently used as an aid in identification of reactive organic as well as ionic species. The theoretical ^{13}C and ^{1}H chemical shifts are calculated from B3LYP/6-311++G(d,p) using GIAO method [45]. For a typical organic molecule the ^{13}C NMR chemical shift range is usually >100 [46]. In most cases, highly shielded atoms appear at downfield and vice versa. The calculated chemical shift values by the DFT theoretical method values well coincides with the experimental values. The calculated chemical shift of the carbon atoms bonded with oxygen and nitrogen with a double bond was identified from 141.8961 - 201.6291 ppm and correspondingly the experimental shifts were observed from 143.176 - 170.863 ppm. The chemical shift values of protons on carbon of a methyl group was expected to be in the range 2 - 5 ppm[47]. The observed theoretical chemical shift of ^{1}H are from 2.1228 - 10.0759 ppm is complemented with the experimental finding from 2.041 - 8.564ppm. Apart from that, deviations are due to the fact that the theoretical calculations are done in gaseous phase while experimental results belong to molecules in solid state.

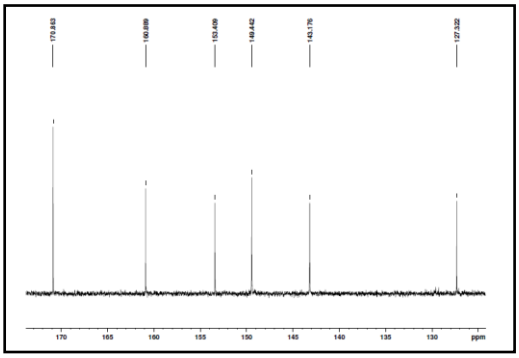

Fig. 7. Experimental ^{13}C NMR spectrum of FCV

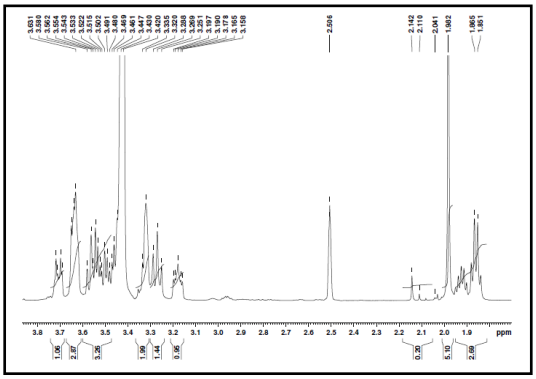

Fig. 8. Experimental ^{1}H NMR spectrum of FCV

Table 7.Theoretical and experimental 13C and 1H isotropic chemical shifts for FCV molecule

Atoms	Experimental	Calculated chemical shifts (ppm)
1C	170.863	178.2227
2C	21.039	16.221
5C	60.836	49.0914
6C	39.385	29.251
7C	34.927	22.1988
8C	40.053	36.0699
12C	153.409	156.2089
16C	160.889	164.2623
17C	143.176	141.8941
19C	61.013	49.2204
23C	28.276	17.6043
24H	2.041	2.1863
25H	1.982	2.1258
26H	5.014	5.0502
28H	6.351	5.6368
29H	2.11	2.2633
30H	3.158	2.4619
31H	1.851	1.9592
32H	6.359	5.7422
33H	4.188	4.2608
35H	8.564	10.0759
36H	5.125	5.5284
37H	6.484	6.0277
38H	4.814	4.7909
39H	5.120	5.1851
40H	2.506	2.4567
41H	3.165	2.4963
42H	1.865	2.1228

Thermodynamic calculations

On the basis of vibrational analysis and statistical thermodynamics, the standard thermodynamic functions of heat capacity (C_p) entropy (S) and enthalpy changes (H) for the title molecule were obtained from the theoretical harmonic frequencies by using perl script THERMO.PL[48], and are listed in Table 8. From Table 8, it can be observed that these thermodynamic functions increase with temperature in the range of 100 to 1000 K, due to the fact that the molecular vibrational intensities increase with increase in temperature.

The correlation equations between heat capacity, entropy, enthalpy changes and temperatures were fitted by quadratic formulae, and the corresponding fitting factors (*R*2) for these thermodynamic properties are 1.0000, 0.999 and 0.999, respectively. The corresponding fit equations are as follows, the correlation graphs are shown in Figure 9.

$$C_{p,m} = 42.03 + 1.222T - 4.810\times10^{-4}T^2 \qquad R = 0.999$$

$$S = 323.0 + 1.437T - 3.489\times10^{-4}T^2 \qquad R = 0.999$$

$$H = -13.33 + 0.1623T + 3.4972\times10^{4}T^2 \qquad R = 0.9995$$

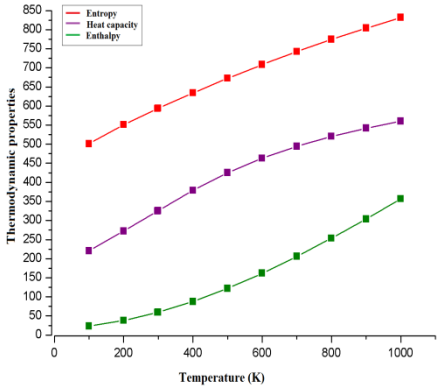

Fig . 9. Correlation plot of thermodynamic properties of the title compound

Table 8.Thermodynamic functions of the title compound

T(K)	S^0_m (J/ mol K)	$C^0_{p,m}$ (J/ mol K)	H^0_m (kJ/ mol)
100	456.349	168.456	11.192
200	601.704	261.730	32.695
298	723.906	357.414	63.047
300	726.123	359.239	63.710
400	842.746	454.753	104.478
500	953.466	538.319	154.252
600	1057.939	607.520	211.658
700	1155.991	664.246	275.339
800	1247.845	711.119	344.180
900	1333.932	750.293	417.307
1000	1414.742	783.353	494.035

These data helped to provide information for further study on the title compound in order to analyze the other thermodynamic energies according to the relationships between thermodynamic functions and to estimate the directions of the chemical reactions according to the second law of thermodynamics [49].

Molecular Docking

The molecular docking is used to predict the preferred binding orientation, affinity and activity of drug molecules and their protein targets. The structure of the target protein was obtained from the RCSB in PDB format [50]. The ligand PDB file was generated from the optimized molecular structure of the FCV molecule. The AutoDock Tools graphical user interface [12] was used to remove the ligand and water molecules present in the target proteins, which was also used to add the polar hydrogen, Kollmann and Geisteger charges in the target proteins.

Table 9. Molecular docking parameters of the title compound with Herpes simplex virus(HSV)

Protein	**Bonded residues**	**Intermolecular energy(kcal/mol)**	**Inhibition constant(μmol)**	**Binding energy(kcal/mol)**	**Bond distance(Å)**
HSV chain B	VAL310	-5.68	10.47	-2.70	2.211
	GLU474	-5.66	10.82	-2.68	2.224
	GLY466	-5.28	20.85	-2.29	2.147
	PRO302	-4.81	45.89	-1.83	1.955
HSV chain C	GLU347,ARG340	-5.69	10.35	-2.71	2.235, 1.988
	GLU458	-4.54	71.79	-1.56	1.775
	ALA354	-4.42	87.98	-1.44	2.196
	THR491	-4.35	100.03	-1.36	2.002

AutoDock results indicate the binding position and bound conformation of the peptide, together with a rough estimate of its interaction [51]. The molecular docking binding energies (kcal/mol) and inhibition constants (mm) with two different chains of the target protein were also obtained and listed in Table 9. Among them, chain C exhibited the lowest free energy at -2.71kcal/mol. The interactions of the FCV ligand with different residues of the target protein are shown in Fig. 10. These results indicate that the FCV ligand exhibits the lower binding energy and inhibition constant for the targeted protein associated with the Herpes Simplex Virus, indicating the antiviral activity of the compound.

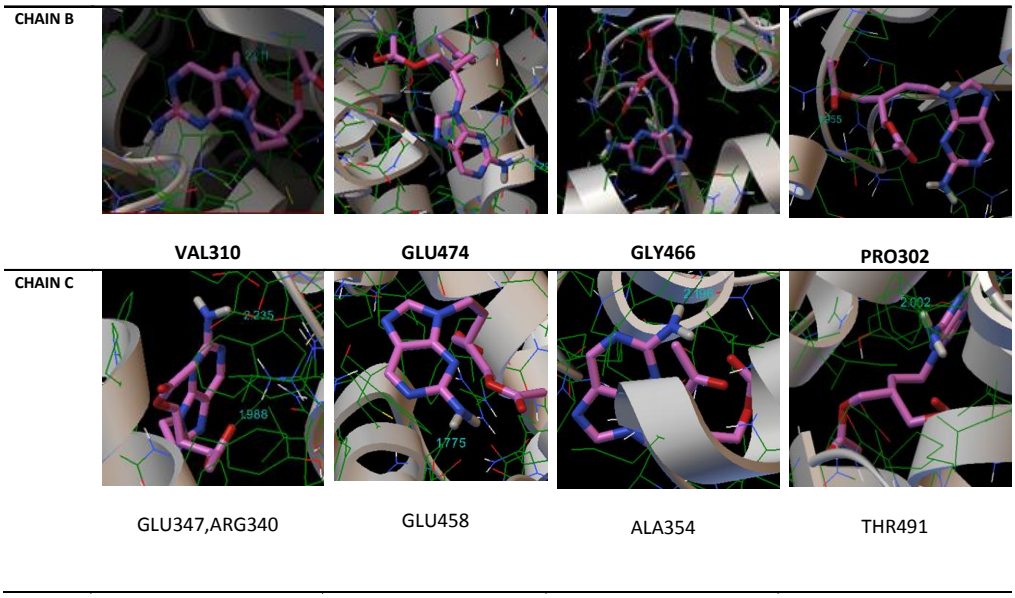

Fig.10. Binding sites of the tiltle compound with HSV virus protein.

Conclusion

In the present work, we have reported on experimental and theoretical spectroscopic analysis of FCV molecule using FT-IR, FT-Raman, UV-Vis and NMR and tools derived from the DFT. In general, a good agreement amid experimental and theoretical normal modes of vibrations was found. The optimized molecular geometry, vibrational frequencies, infrared intensities and Raman activity of the molecule have been calculated by using DFT/B3LYP method with 6-311++G(d,p) basis set. The λ_{max}, band gap energy were also calculated and compared with the experimental UV-Vis spectrum. The chemical shifts were compared with experimental data in DMSO solution, showing a very good agreement both for Carbon (^{13}C) and proton (^{1}H) NMR. FMOs analysis reveals the presence of ICT within the molecule. The possible electrophilic and nucleophilic reactive sites of the molecule were predicted and the intramolecular interactions of the molecule were also confirmed through NBO analysis. All the theoretical results show good agreement

with experimental data. The band energy gap calculated from HOMO and LUMO analysis gives significant information about the title compound. Reactive sites of the title compound were investigated from MEP and Fukui function analysis. In addition, the molecular docking output shows that the title compound acts as a good antiviral agent with low binding energy of -2.7kcal/mol.

Reference

[1] Yurdaydin, C. Bozkaya, H. Gurel, S. Tillmann, H.L. Aslam, N. Heper, A.O. Erden, E. Yalcin, K. Iliman, N. Uzunalimoglu, O. Manns, M.P. Bozday, A.M. Famciclovir treatment of chronic delta hepatitis, *Journal of hepatology,* 37(2) (2002) 266-271.

[2] Cirelli, R. Herne, K. McCrary, M. Lee, P. Tyring, S.K. Famciclovir: Review of clinical efficacy and safety, *Antiviral Research*, 29 (1996) 141-151.

[3] Budavari, S. The Merck Index, 13th ed., An Encyclopedia of chemicals, drugs and biological, Division of Merck and Co., Inc., Rahway New Jersey, USA (2001) 3960.

[4] Amaku Friday James, Otuokree Ifeanyi Edozie, I gwe Kalu Kalu, Conformational analysis and excited – state properties of a highly potent aniviral drug, 2-[(acetyloxy)methyl]-4-(2-amino-7H-pyrrolo[3,2-d]pyrimidin-7-yl)butyl acetate (famciclovir), *IJSEAS*, 1(9) (2015) 66-72.

[5] Akmal S. Gaballa, Said M. Teleb, El-Metwally Nour, Preparation and spectroscopic studies on charge-transfer complexes of famciclovir drug with different electron acceptors, *Journal of Molecular Structure*, 1024 (2012) 32-39.

[6] Becke, A.D. Density-functional thermochemistry. III. The role of ecxact exchange, *Journal of Chemical Physics*, 98(1993) 5648-5652.

[7] Frisch, M.J. Trucks, G.W. Schlegel, H.B. Scuseria, G.E. Robb, M.A. Cheeseman, J.R. Scalmani, G. Barone, V. Mennucci, B. Petersson, G.A. Nakatsuji, H. Caricato, M. Li, X. Hratchian, H.P. Izmaylov, A.F. Bloino, J. Zheng, G. Sonnenberg, J.L. Hada, M Ehara, M. Toyota, K. Vreven, T. Montgomery, J.A. Perlta, J.E. Ogliaro, F. Bearpark, M. Heyd, J.J. Brothers, E. Kudin, K.N. Staroverov, V..N. Kobayashi, R. Normand, J. Raghavachari, K. Rendell, A. Burant, J.C. Iyengar, S.S. Tomasi, J. Cossi, M. Rega, N.Millam, J.M. Klene, M. Knox, J.E. Cross, J.B. Bakken, V. Adamo, C. Jaramillo, J. Gomperts, R. Stratmann, R.E. Yazyev, O. Austin, A.J. Cammi, R. Pomelli, C. Ochterski, J.W. Martin, R.J. Morokuma, K. Zakrzewski, V.G. Voth, G.A. Salvador, P. Dannenberg, J.J. Dapprich, S. Daniels, A.D. Farkas, O. Foresman, J.B. Ortiz, J.V. Ciolslowski, J. Fox, D.J. Gaussian 09, Revision E.01, Gaussian, Inc., Wallingford CT, 2009.

[8] Jomroz, M.H. Vibrational Energy Distribution Analysis, VEDA4, 2004, Warsaw.

[9] Kereztury, G. Holly S, Varga, J. Besenyei, G. Wang, A.Y. During, J.R. Vibrational spectra of monothiocarbomates-ii. IR and Raman spectra, vibrational assignment, conformational analysis and ab initio calculations of S-methyl-N,Ndimethylthiocarbamate, *Spectrochim. Acta A* 49 (1993) 2007-2026.

[10] Keresztury, G. Chalmers, J.M. Griffith, P.R. (Eds.), Raman Spectroscopy: Theory in Hand Book of Vibrational Spectroscopy, 1, John Wiey &Sons Ltd, New York, 2002.
[11] Wolinski, K. Haacke, R. Hinton, J.F. Pulay, P. Methods for parallel computation of SCR NMR chemical shifts by GAIO method: efficient integral calculation, multi-Fock algorithm, and pseudodiagonalization, *Journal of Computatioal Chemistry*, 18(6) (1997)c816-825.
[12] Morris, G.M. Goodsell, D.S. Halliday, R.S. Huey, R. Hart, W.E. Belew, R.K. Olson, A.J. Automated Docking Using a Lamarckian Genetic Algorithm and Empirical Binding Free Energy Function, *J. Comput. Chem*. 19 (1998) 1639-1662.
[13] Silverstein, M. Bassler, G.C. Morril, C. Spectro-scopic Identification of Organic Compounds, Fifth ed., John Wiley & Sons Inc., Singapore, 1991.
[14] Wilson, E.B. Decius, J.C. Cross, P.C. Molecular Vibrations, Dover Publications Inc., New York, 1980.
[15] Socrates, G. Infrared and Raman Characteristic Group Frequencies. Tables and charts. 3rd ed., John Wiley, New York 2001.
[16] Colthup, N.B. Daly, L.H. Wiberley, S.E. Introduction to Infrared and Raman Spectroscopy, Academic Press, New York, 1990.
[17] Dollish, F.R. Fateley, W.G. Benteley, F.F. Characteristic Raman Frequencies of Organic compounds, Wiley, New York (1997).
[18] Varasanyi, G. Vibrational Spectra of Benzene Derivatives, Academic Press, New York, 1969.
[19] Jamroz, M.H. Dobrowolski, J.Cz. Brzozowski, R. Vibrational modes of 2,6-,2,7-, and 2,3-diiso-propylnaphthalene. A DFT study, *Journal of molecular structure*, 787 (2006) 172-183.
[20] Muthu, S. Prabhakaran, A. Vibrational spectroscopic study and NBO analysis on tranexamic acid using DFT mmethod, *Spectrochim. Acta A*, 129 (2014) 184-192.
[21] Monirah A. Al-Alshaikh, S. Muthu, S. Ebtehal, S. Al-Abdullah, E. Elamurugu Porchelvi, Siham Lahsasni, Ali, A. El-Emam, Structural and spectroscopic characterization of n′-[(1e)-(4-fluorophenyl)methylidene]thiophene-2-carbohydrazide, a potential precursor to bioactive agents, *Macedonian Journal of Chemistry and Chemical Engineering*, 35(1) (2016) 63–77.
[22] Arjunan, V., Ravindran, P., Subhalakshmi, K., Mohan, S., Synthesis, structural, vibrational and quantum chemical investigations of N-(2-methylphenyl)-2,2-dichloroacetamide and N-(4-methylphenyl)-2,2-dichloroacetamide, *Spectrochim. Acta A*, 74 (2009) 607–616.
[23] Arjunan, V., Senthilkumari, S., Ravindran, P., Mohan, S., Synthesis, FTIR and FT-Raman spectral analysis and structure–activity relations of N-(4-bromophenyl)-2,2-dichloroacetamide by DFT studies, *J. Mol. Struct*., 1064 (2014) 15–26.
[24] Varsanyi, G., 1974. Assignments for Vibrational Spectra of Seven Hundred Benzene Derivatives vol. I. Adam Hilger, London.
[25] Socrates, G., 2001. Infrared and Raman Characteristic Group Frequencies. 3rd edition. John Wiley & Sons, Ltd., New York.

[26] Snehalatha, M., Ravikumar, C., Sekar, N., Jayakumar, V.S., Hubert Joe, I., FT-Raman, IR and UV-visible spectral investigations and ab initio computations of a nonlinear food dye amaranth, *J. Raman Spectrosc*., 39 (2008) 928–936.
[27] Arul Dhas, D., Hubert Joe, I., Roy, S.D.D., Balachandran, S., Spectroscopic investigation and hydrogen-bonding analysis of triazinones. *J. Mol. Model*., 18 (2012) 3587–3608.
[28] Kosar B, Albayrak C, Spectrochim. Spectroscopic investigations and quantum chemical computational study of (E)-4-methoxy-2-[(p-tolylimino)methyl]phenol, *Spectrochim. Acta A*, 87 (2011) 160-167.
[29] Szafran, M. Komasa, A. Adamska, E.B. Crystal and molecular structure of 4-carboxypiperidinium chloride (4-piperidinecarboxylic acid hydrochloride), *J. Mol. Struct. THEOCHEM*, 827 (2007) 101-107.
[30] Ramesh, A. Gunasekaran, S. Ramkumar, R. Molecular structure, Vibrational Spectra, UV-Visible and NMR Spectral Analysis on Ranitidine Hydrochloride using AB Initio and DFT Methods, *Int. J. Current Reaseach Aca. Rev*. 3(11) (2015) 117-138.
[31] Parr, R.G. Yang, W. Functional Theory of Atoms and Molecules, Oxford University press, New York, 1989.
[32] Ayers, P.W. Parr, R.G. Parr, Variational principals for describing chemical reactions: The Fukui function and chemical hardness revisted, *J. Am. Chem. Soc*. 122 (2000) 2010–2018.
[33] Renuga, S. Karthikesan, M. Muthu, S. FTIR and Raman spectra, electronic spectra and normal coordinate analysis of N,N-dimethyl-3-phenyl-3-pyridin-2-yl-propan-1-amine by DFT method, *Spectrochim. Acta A* 127 (2014) 439–453.
[34] Chattaraj, P.K. Maiti, B. Sarkar, U. Philicity: A unified treatment of chemical reactivity and selectivity, *J. Phys. Chem. A* 107 (2003) 4973–4975.
[35] Morell, C. Grand, A. Toro-Labbe, A. New dual descriptor for chemical reactivity, *J. Phys. Chem. A*, 109 (2005) 205–212.
[36] Scrocco, E. Tomasi, J. Electronic Molecular Structure, Reactivity and Intermolecular Forces: An Euristic Interpretation by Means of Electrostatic Molecular Potentials, *Adv. Quantum Chem.* 11 (1978) 115-193.
[37] Luque, F.J. Lopez, J.M. Orozco, M.
[38] Muray, J.S. Sen, K. Perspective on "electrostatic interactions of a solute with a continuum. A direct utilization of ab initio molecular potentials for the prevision of solvent effects", *Theor. Chem. Acc*. 103 (2000) 343-345.
[39] Seminario, J.M. Molecular Electrostatic Potentials. Concepts and Applications, Elsevier, Amsterdam, 1996.
[40] Fleming, I., Frontier Orbitals and Organic Chemical Reactions. JohnWiley and Sons, New York (1976).
[41] Tamer, Ö., Sariboga, B., Ibrahim Uçar, A combined crystallographic, spectroscopic, antimicrobial, and computational study of novel dipicolinate copper(II) complex with 2-(2-hydroxyethyl)pyridine, *Struct. Chem.* 23 (2012) 659–670.

[42] Çirak, Ç., Koç, N., A combined crystallographic, spectroscopic, antimicrobial, and computational study of novel dipicolinate copper(II) complex with 2-(2-hydroxyethyl)pyridine, *J. Mol. Model*. 18 (2012) 4453–4464.
[43] Subramanian, N. Sundarganesan, N. Jayabharathi, J. Molecular structure, spectroscopic (FT-IR, FT-Raman, NMR, UV) studies and first-order molecular hyperpolarizabilities of 1,2-bis(3-methoxy-4-hydroxybenzylidene)hydrazine by density functional method, *Spectrochim. Acta A* 76 (2010) 259-269.
[44] Sarojini, K. Krishnan, H. Kanakam, Charles, C. Muthu, S. Synthesis, structural, spectroscopic studies, NBO analysis, NLO and HOMO-LUMO of 4-methyl-N-(3-nitrophenyl)benzene sulfonamide with experimental and theoretical approaches, *Spectrochimica Acta A* 108 (2013) 159-170.
[45] Muthu, S. Ramachandran, G. Uma Maheswari, J. Vibrational spectroscopic investigation on the structure of 2-ethylpyridine-4-carbothioamide, *Spectrochimica Acta A* 93(2012) 214-222.
[46] Socrates, G. Infrared Characteristic Group Frequencies, John Wiley Interscience, New York, 1980.
[47] Robert M. Silverstein, Francis X. Webster, David J. Kiemle, Spectrometric identification of organic compounds, seventh edition,, John Wiley and sons, Inc. New York, 2005.
[48] Irikura K.K. THERMO, PL (National Institute of Standards and Technology), Gaithersburg, MD, 2002
[49] Leena Sinha, Mehmet Karabacak, Narayan, V. Mehmet Cinar, Onkar Prasad, Molecular structure, electronic properties, NLO, NBO analysis and spectroscopic characterization of Gabapentin with experimental (FT-IR and FTRaman) techniques and quantum chemical calculations, *Spectrochim. Acta A* 109 (2013) 298-307.
[50] http://www.rcsb.org/pdb.
[51] Raja, M. Raj Muhamed, R. Muthu, S. Suresh, M. Muthu, K. Synthesis, spectroscopic (FT-IR, FT-Raman, NMR, UV-Visible), Fukui function, antimicrobial and molecular docking study of (E)-1-(3-bromobenzylidene)semicarbazide by DFT method, *Journal of Molecular Structure* , 1130 (2017) 374-384.